

Efficient methods for solving water flow in variably saturated soils under prescribed flux infiltration

Xiaoxian Zhang^{a,*}, A. Glyn Bengough^a, John W. Crawford^b, Iain M. Young^b

^a*Soils, Plants and Environment Division, Scottish Crop Research Institute, Invergowrie, Dundee DD2 5DA, UK*

^b*SIMBIOS Centre, University of Abertay, Dundee DD1 1HG, UK*

Received 10 May 2001; revised 5 November 2001; accepted 26 November 2001

Abstract

The non-linear solvers in numerical solutions of water flow in variably saturated soils are prone to convergence difficulties. Many aspects can give rise to such difficulties and in this paper we address the gravity term and the prescribed-flux boundary in the Picard iteration. The problem of the gravity term in the Picard iteration is iteration-to-iteration oscillation as the gravity term is treated, by analogy with the time-step advance technique, ‘explicitly’ in the iteration. The proposed method for the gravity term is an improvement of the ‘implicit’ approach of Zhang and Ewen [Water Resour. Res. 36 (2000) 2777] by extending it to heterogeneous soil and approximating the inter-nodal hydraulic conductivity in the diffusive term and the gravity term with the same scheme. The prescribed-flux boundary in traditional methods also gives rise to iteration-to-iteration oscillation because there is no feedback to the flux in the solution at the new iteration. To reduce such oscillation, a new method is proposed to provide such a feedback to the flux. Comparison with traditional Picard and Newton iteration methods for a wide range of problems show that a combination of these two proposed methods greatly improves the stability and consequently the computational efficiency, making the use of small time step and/or under-relaxation solely for convergence unnecessary. © 2002 Elsevier Science B.V. All rights reserved.

Keywords: Richards’ equation; Variably saturated flow; Iteration method; Numerical method

1. Introduction

Numerical modeling of water flow in variably saturated soils is needed in a wide range of applications and is often based on the Richards’ equation (Richards, 1931). For stability consideration, most of the existing approaches solve the equation with a fully implicit approach and use pressure head, which is continuous in both saturated and unsaturated zones, as primary

variable. This requires estimates of soil hydraulic properties at the new time level, giving a non-linear system that has to be solved by iteration. Under certain situations, especially those involving sharp wetting fronts and perched water tables, the iteration is prone to convergence difficulties. This presents one of the most significant challenges in numerical solution of variably saturated flow. Although considerable effort has been expended over the last few decades (e.g. Cooley, 1983; Ross, 1990; Zaidel and Russo, 1992; Li, 1993; Paniconi and Putti, 1994; Forsyth et al., 1995; Pan and Wierenga, 1995, 1997; Tocci et al., 1997; Miller et al., 1998), some issues remain unresolved (Williams and Miller, 1999).

* Corresponding author. Address: Soil–plant Dynamics Unit, Scottish Crop Research Institute, Invergowrie, Dundee, DD2 5DA, UK. Fax: +44-1382-562426.

E-mail address: x.zhang@scri.sari.ac.uk (X. Zhang).

The iteration methods that are routinely used are based on the Picard and Newton techniques. Theoretically, the Newton method converges one order faster than the Picard method, but under some situations, the Picard method is more efficient than the Newton method (Paniconi and Putti, 1994). The Newton method converges quadratically only in the vicinity of the solution. When the estimated values used to form the Jacobian matrix is not near the solution, the Newton method is likely to give rise to severe non-physical oscillation in the iteration and diverge consequently because under this situation, the high-order terms neglected in the Taylor series expansion, which contribute to the right-hand side vector of the linear system, are still significant and the Jacobian matrix is devoid of diagonal dominance. The Picard method has a diagonally dominant matrix, but still gives rise to the iteration-to-iteration oscillation that causes divergence. An important factor that affects the convergence of the Picard method is the gravity term as it is treated, in analogy with the time-step advance technique, ‘explicitly’ in the iteration, whilst a robust method requires ‘implicit’ approach. An improvement in the convergence is related to an improvement in stability. For example, some common approaches such as the reduction of time step, the use of under-relaxation and the mass-lumped technique (Neuman, 1973) are methods to improve the stability by enhancing the diagonal terms of the matrix of the linear system. Several methods such as line search methods (Pan and Wierenga, 1997; Williams et al., 2000) are available for searching the optimal relaxation factors, but they are expensive. The use of small time steps for convergence is time-consuming.

The prescribed-flux boundary is also a factor that may cause convergence difficulties in solving variably saturated flow with the pressure head as primary variable, especially when the flux is relatively large to soil permeability and the soil is dry. This is because under these situations, the elements related to the boundary node in the matrix of the linear system are small and unable to transmit the water away from the boundary node quickly. As a result, the water dumps itself at the boundary node, resulting in the pressure head out physical bounds. One way to alleviate this problem is to provide a proper feedback in the matrix to the flux to keep the result in the physical bounds. The purpose of this paper is to provide such a feedback.

Combined with an improved method for the gravity term based on the implicit approach of Zhang and Ewen (2000), the new method greatly reduces the iteration-to-iteration oscillation and improves the computational efficiency, which eliminates the need for small time steps and/or under-relaxation for convergence.

2. Methods

A combination of the mass balance and Darcy’s law gives the Richards’ equation, which in one dimension is (Richards, 1931):

$$\frac{\partial \theta}{\partial t} = \frac{\partial}{\partial z} \left(K \frac{\partial h}{\partial z} \right) + \frac{\partial K}{\partial z} \quad (1)$$

where θ is volumetric water content, K is hydraulic conductivity, h is pressure head, t is time and z is elevation. With appropriate boundary and initial conditions, Eq. (1) is solved by a fully implicit, node-centred and mass-lumped finite volume approach. Solving the time derivative term by the method of Celia et al. (1990) and the diffusive term by the Picard iteration gives:

$$\begin{aligned} & \frac{(\Delta z_{i-1} + \Delta z_i)(\theta_i^{k+1,m} - \theta_i^k)}{2\Delta t} \\ & + \frac{(\Delta z_{i-1} + \Delta z_i)}{2\Delta t} \frac{\partial \theta}{\partial h} \Big|_i^{k+1,m} (h_i^{k+1,m+1} - h_i^{k+1,m}) \\ & = K_{i-1/2}^{k+1,m} \frac{(h_{i-1}^{k+1,m+1} - h_i^{k+1,m+1})}{\Delta z_{i-1}} \\ & + K_{i+1/2}^{k+1,m} \frac{(h_{i+1}^{k+1,m+1} - h_i^{k+1,m+1})}{\Delta z_i} \\ & + (K_{1+1/2}^{k+1,m+1} - K_{1-1/2}^{k+1,m+1}) \end{aligned} \quad (2)$$

where $K_{i\pm 1/2}$ are the inter-nodal hydraulic conductivities between node z_i and nodes $z_{i\pm 1}$, respectively, and are approximated by the following integral average:

$$K_{i\pm 1/2} = \begin{cases} \frac{1}{h_{i\pm} - h_i} \int_{h_i}^{h_{i\pm 1}} K(h) dh & h_i \neq h_{i\pm 1} \\ K(h_{i\pm 1}) & h_i = h_{i\pm 1} \end{cases} \quad (3)$$

The integral average has proved to be an accurate

approximation of the inter-nodal hydraulic conductivity (Zaidel and Russo, 1992; Li, 1993). For complicated $K(h)$ such as the van Genuchten formula the integral (3) is approximated numerically by:

$$K_{i-1/2} = \sum_{j=1}^L w_j K_D(h_j) \quad h_j = \lambda_j h_i + (1 - \lambda_j) h_{i-1},$$

$$K_{i+1/2} = \sum_{n=1}^L w_n K_U(h_n) \quad h_n = \lambda_n h_{i+1} + (1 - \lambda_n) h_i, \quad (4)$$

$$\sum_{j=1}^L w_j = \sum_{n=1}^L w_n = 1$$

where $0 \leq \lambda_j \leq 1$, $0 \leq \lambda_n \leq 1$, $0 \leq w_j \leq 1$ and $0 \leq w_n \leq 1$ are weighting factors; the subscripts D and U represent the values taken from the cells $[z_{i-1}, z_i]$ and $[z_i, z_{i+1}]$ respectively, when the materials in the two cells are different in a heterogeneous soil. As proved in Appendix A, the above Picard iteration for the diffusive term can be derived from a chord–slope method, which does not have the quadratic convergence rate near the solution that the full Newton iteration has, but converges faster than the Picard iteration for the gravity that converges linearly.

2.1. Approach to the gravity term

To improve the Picard-iteration’s stability, Zhang and Ewen (2000) proposed to calculate the gravity term implicitly during the iteration using an upwind or a central scheme. Their method approximated the inter-nodal hydraulic conductivity in the diffusive term and the gravity term differently, as a result, it does not converges to the same solution as the Picard method that approximated the inter-nodal hydraulic conductivity in the diffusive term and the gravity term with the same approach. Here we improve their method by approximating the inter-nodal hydraulic conductivity in the diffusive term and the gravity term by the same integral average given in Eq. (3) and extending it to heterogeneous soil. The last term on the right-hand side of Eq. (2) arises from the discretization of the gravity term. With the two inter-nodal conductivities estimated by Eq. (4), we add and subtract two same terms, $K_D(h_i^{k+1,m+1})$ and $K_U(h_i^{k+1,m+1})$, to the discretization of the gravity term

as follows:

$$K_{i+1/2}^{k+1,m+1} - K_{i-1/2}^{k+1,m+1}$$

$$= \sum_{n=1}^M w_n \left\{ K_U \left[\lambda_n h_{i+1}^{k+1,m+1} + (1 - \lambda_n) h_i^{k+1,m+1} \right] - K_U \left(h_i^{k+1,m+1} \right) \right\} - \sum_{n=1}^M w_n \left\{ K_D \left[\lambda_n h_i^{k+1,m+1} + (1 - \lambda_n) h_{i-1}^{k+1,m+1} \right] - K_D \left(h_i^{k+1,m+1} \right) \right\}$$

$$+ K_U \left(h_i^{k+1,m+1} \right) - K_D \left(h_i^{k+1,m+1} \right) \quad (5)$$

As in Zhang and Ewen (2000), each pair of the hydraulic conductivities in the brace bracket of Eq. (5) are calculated from:

$$K_U \left[\lambda_n h_{i+1}^{k+1,m+1} + (1 - \lambda_n) h_i^{k+1,m+1} \right] - K_U \left(h_i^{k+1,m+1} \right)$$

$$= \tan(\alpha_n) \lambda_n \left(h_{i+1}^{k+1,m+1} - h_i^{k+1,m+1} \right),$$

$$K_D \left[\lambda_n h_i^{k+1,m+1} + (1 - \lambda_n) h_{i-1}^{k+1,m+1} \right] - K_D \left(h_i^{k+1,m+1} \right)$$

$$= \tan(\beta_n) (1 - \lambda_n) \left(h_{i-1}^{k+1,m+1} - h_i^{k+1,m+1} \right) \quad (6)$$

where α_n and β_n are the angles in the $K(h) \sim h$ coordinate formed between the h axis and the lines that link $K_U[\lambda_n h_{i+1}^{k+1,m+1} + (1 - \lambda_n) h_i^{k+1,m+1}]$ and $K_U[h_i^{k+1,m+1}]$, and $K_D[\lambda_n h_i^{k+1,m+1} + (1 - \lambda_n) h_{i-1}^{k+1,m+1}]$ and $K_D[h_i^{k+1,m+1}]$, respectively. The slopes in Eq. (6) are simply approximated by their values at the previous iteration:

$$\tan(\alpha_n) = \frac{K_U \left[\lambda_n h_{i+1}^{k+1,m} + (1 - \lambda_n) h_i^{k+1,m} \right] - K_U \left(h_i^{k+1,m} \right)}{\lambda_n \left(h_{i+1}^{k+1,m} - h_i^{k+1,m} \right)},$$

$$\tan(\beta_n) = \frac{K_D \left[\lambda_n h_i^{k+1,m} + (1 - \lambda_n) h_{i-1}^{k+1,m} \right] - K_D \left(h_i^{k+1,m} \right)}{(1 - \lambda_n) \left(h_{i-1}^{k+1,m} - h_i^{k+1,m} \right)} \quad (7)$$

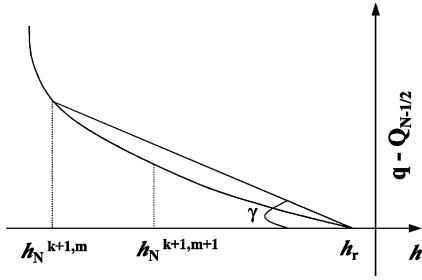


Fig. 1. Schematic illustration of the relationship between $q - Q_{N-1/2}^{k+1}$ and h_N^{k+1} on a flux-prescribed boundary, and the new method to calculate them.

With the slopes calculated by Eq. (7), Eq. (6) performs implicitly in the iteration. As the implicit approach adds helpful feedback to the gravity calculation at the new iteration, it improves the solution stability. The method for the gravity term is applied only to the nodes where the denominator in Eq. (7) is not zero, otherwise the standard Picard method is used. The last two terms on the right-hand side of Eq. (5) sum to zero when materials in the two cells are the same. When materials in the two cells are different, the two terms can be Taylor expanded around their values at level m to make a Newton iteration, but our experiences show that this does not result in a noticeable improvement over by simply approximating them with their values at level m .

2.2. Approach to the prescribed-flux boundary

We assume that node N is a surface node where a flux, q , is prescribed. Application of Eq. (2) to this node gives:

$$\begin{aligned} & \frac{K_{N-1/2}^{k+1,m}}{\Delta z_N} (h_N^{k+1,m+1} - h_N^{k+1,m+1}) \\ & - \frac{\Delta z_N}{2\Delta t} \frac{d\theta}{dh} \Big|_N^{k+1,m} h_N^{k+1,m+1} - K_{N-1/2}^{k+1,m+1} \\ & = \frac{\Delta z_N (\theta_N^{k+1,m} - \theta_N^k)_D}{2\Delta t} - \frac{\Delta z_N}{2\Delta t} \frac{d\theta}{dh} \Big|_N^{k+1,m} h_N^{k+1,m} - q \end{aligned} \tag{8}$$

where $z_n > z_{n-1}$ is assumed, and the infiltration rate q is positive. The calculation of q using Eq. (8) can give rise to iteration-to-iteration oscillation when q is relatively large and the node N is dry because under these

situations, the coefficients on the left-hand side of Eq. (8) are small and provide no direct feedback to q to keep the solution within physical bounds in the iteration. To provide a proper feedback, let us see how h_N responds to q when q is a constant. Denoting the flux at the bottom ($z_{N-1/2}$) of the control domain of the node N as $Q_{N-1/2}$ (assumed positive), then $q > Q_{N-1/2}$ until flow in cell $[z_{n-1}, z_n]$ reaches steady state. If h_r is the pressure head at the node N when $q = Q_{N-1/2}$, it can be seen from Fig. 1 that $q - Q_{N-1/2}^{k+1}$ can be expressed as:

$$q - Q_{N-1/2}^{k+1} = \tan(\gamma) (h_N^{k+1} - h_r) \tag{9}$$

where γ is an angle as shown in Fig. 1. Approximating $\tan(\gamma)$ by its value at the previous iteration gives:

$$\begin{aligned} & (q - Q_{N-1/2})^{k+1,m+1} \\ & = \frac{q}{h_N^{k+1,m} - h_r} (h_N^{k+1,m+1} - h_r) \\ & - \frac{Q_{N-1/2}^{k+1,m}}{h_N^{k+1,m} - h_r} (h_N^{k+1,m+1} - h_r) \end{aligned} \tag{10}$$

The last term on the right-hand side of Eq. (10) is an approximation of the flux at $z_{N-1/2}$ and is approximated by its value at the new iteration

$$\begin{aligned} & \frac{Q_{N-1/2}^{k+1,m}}{h_N^{k+1,m} - h_r} (h_N^{k+1,m+1} - h_r) \\ & = \frac{K_{N-1/2}^{k+1,m}}{\Delta z_N} (h_N^{k+1,m+1} - h_N^{k+1,m+1}) + K_{N-1/2}^{k+1,m+1} \end{aligned} \tag{11}$$

Eq. (10) then reduces to:

$$q^{k+1,m+1} = \frac{q}{h_N^{k+1,m} - h_r} (h_N^{k+1,m+1} - h_r) \tag{12}$$

In the proposed method q in Eq. (8) is replaced by $q^{k+1,m+1}$ in Eq. (12). The above development assumed that the reference pressure head h_r is the pressure head at the node N when $q = Q_{N-1/2}$, but this is not essential because of the use of Eq. (12). As will be seen in Section 3, given h_r larger than the pressure head at node N when $q = Q_{N-1/2}$, the use of Eq. (12) gives stable solution because under this situation $\tan(\gamma)$ in Eq. (9) is positive, which improves the stability because of the way that the prescribed-flux is linked to the matrix of the linear system through Eq. (12). The

use of Eq. (12) does not introduce additional errors because its two sides are equal after convergence.

3. Examples

Numerical simulations were conducted for a number of examples to examine the accuracy and improvement of the proposed methods over traditional methods. The proposed method for the flux boundary can be applied to the Picard and Newton methods, but is less effective in the Newton method than in the Picard method because the oscillation in the Newton method is mainly caused by the method itself. Each flow example was first simulated by three basic methods with the flux boundary treated by the standard method: (1) (MPI) the modified Picard iteration of Celia et al. (1990); (2) (Newton) the Newton iteration derived in Appendix A, which is equivalent to the method of Li (1993); (3) (IMPI) a combination of the Picard iteration for the diffusive term and the proposed iteration for the gravity term. We then simulated each example again by the three basic methods with the flux boundary treated by the proposed method, which will be called as z-methods and referred to as ZMPI, Znewton and ZIMPI, respectively. The linear system of each method was solved with the pressure head increment, $\delta h^{k+1,m+1} = h^{k+1,m+1} - h^{k+1,m}$, as primary variable:

$$\begin{aligned}
 &A_i^{k+1,m} \delta h_{i-1}^{k+1,m+1} \\
 &\quad - \left(a_i^{k+1,m} + B_i^{k+1,m} + d_i^{k+1,m} \right) \delta h_i^{k+1,m+1} \\
 &\quad + D_i^{k+1,m} \delta h_{i+1}^{k+1,m+1} \\
 &= R_i^{k+1,m}, \\
 &R_i^{k+1,m} = \frac{(\Delta z_{i-1} + \Delta z_i) (\theta_i^{k+1,m} - \theta_i^k)}{2\Delta t} \\
 &\quad - \frac{K_{i-1/2}^{k+1,m}}{\Delta z_{i-1}} (h_{i-1}^{k+1,m} - h_i^{k+1,m}) \\
 &\quad - \frac{K_{i+1/2}^{k+1,m}}{\Delta z_i} (h_{i+1}^{k+1,m} - h_i^{k+1,m}) - K_{i+1/2}^{k+1,m} \\
 &\quad + K_{i-1/2}^{k+1,m} - q \delta_{iN}
 \end{aligned} \tag{13}$$

where δ_{iN} is the Kronecker delta. $B_i^{k+1,m}$ in MPI, Newton and IMPI are the same

$$B_i^{k+1,m} = \frac{(\Delta z_{i-1} + \Delta z_i)}{2\Delta t} \left. \frac{\partial \theta}{\partial h} \right|_i^{k+1,m} \tag{14}$$

and in the MPI, ZMPI, IMPI and ZIMPI, $a_i^{k+1,m} = A_i^{k+1,m}$ and $d_i^{k+1,m} = D_i^{k+1,m}$, which are:

in the MPI and ZMPI,

$$A_i^{k+1,m} = \frac{K_{i-1/2}^{k+1,m}}{\Delta z_{i-1}}, \quad D_i^{k+1,m} = \frac{K_{i+1/2}^{k+1,m}}{\Delta z_i} \tag{15}$$

and in the IMPI and ZIMPI,

$$A_i^{k+1,m} = \frac{K_{i-1/2}^{k+1,m}}{\Delta z_{i-1}} + \sum_{n=1}^L w_n (\lambda_n - 1) \tan(\beta_n), \tag{16}$$

$$D_i^{k+1,m} = \frac{K_{i+1/2}^{k+1,m}}{\Delta z_i} + \sum_{n=1}^L w_n \lambda_n \tan(\alpha_n)$$

In the Newton:

$$\begin{aligned}
 A_i^{k+1,m} &= \frac{K(h_{i-1}^{k+1,m})_D}{\Delta z_{i-1}} - \sum_{j=1}^L w_j (1 - \lambda_j) \left. \frac{\partial K(h)_D}{\partial h} \right|_{h=h_j}, \\
 D_i^{k+1,m} &= \frac{K(h_{i+1}^{k+1,m})_U}{\Delta z_i} + \sum_{n=1}^L w_n \lambda_n \left. \frac{\partial K(h)_U}{\partial h} \right|_{h=h_n}, \\
 a_i^{k+1,m} &= \frac{K(h_i^{k+1,m})_D}{\Delta z_{i-1}} - \sum_{j=1}^L w_j \lambda_j \left. \frac{\partial K(h)_D}{\partial h} \right|_{h=h_j}, \\
 d_i^{k+1,m} &= \frac{K(h_i^{k+1,m})_U}{\Delta z_i} + \sum_{n=1}^L w_n (1 - \lambda_n) \left. \frac{\partial K(h)_U}{\partial h} \right|_{h=h_n}
 \end{aligned} \tag{17}$$

where h_n and h_j are calculated from Eq. (4). The difference between the z-methods and the basic methods is that in the z-methods:

$$B_i^{k+1,m} = \frac{(\Delta z_{i-1} + \Delta z_i)}{2\Delta t} \left. \frac{\partial \theta}{\partial h} \right|_i^{k+1,m} + \frac{q}{(h_r - h_N^{k+1,m})} \delta_{iN} \tag{18}$$

which provides a feedback to the flux boundary. Eq. (18) is applied only when $h_N^{k+1,m} < h_r$, otherwise the flux is treated by the standard method.

The termination of the non-linear iteration was

Table 1

The CPU time of the basic methods and the z -methods for simulating infiltrations into the sand under a single set of infiltration rates (simulation time was 1 day) (F represents iteration failed to converge)

q (m/day)	Δt (day)	MPI	Newton	IMPI	ZMPI	Znewton	ZIMPI
0.5	0.0005	F	F	F	110.4	F	110.5
	0.005	F	F	F	31.4	F	24.9
	0.1	F	F	F	F	F	3.5
1.0	0.0005	F	F	F	133.0	F	133.2
	0.005	F	F	F	51.1	F	35.7
	0.1	F	F	F	F	F	4.5
1.5	0.0005	F	F	F	155.5	F	155.4
	0.005	F	F	F	72.5	F	44.0
	0.1	F	F	F	F	F	5.3

based on the residual $R_i^{k+1,m}$ in Eq. (13). The iteration was assumed to have converged when the $\max |R_i^{k+1,m}|$ calculated over all the nodes was less than 10^{-4} m/day. The iteration for level $k+1$ was launched using the converged solution at k , i.e. $h^{k+1,0} = h^k$, and the integral-average inter-nodal conductivities were calculated by a three-point Simpson formula for which the weighting factors in Eq. (4) are $L = 3$, $w_1 = w_3 = 1/6$, $w_2 = 4/6$, $\lambda_1 = 1$, $\lambda_2 = 0.5$ and $\lambda_3 = 0$.

Three soils were employed in the tests: a sand and a clay taken from Hills et al. (1989), and a loam from van Genuchten (1980). Their van Genuchten parameters are: sand ($\theta_s = 0.3658$, $\theta_r = 0.0286$, $n = 2.239$, $\alpha = 2.80(\text{m}^{-1})$, $K_s = 5.41$ m/day); clay ($\theta_s = 0.4686$, $\theta_r = 0.106$, $n = 1.3954$, $\alpha = 1.04(\text{m}^{-1})$, $K_s = 0.131$ m/day); and loam ($\theta_s = 0.434$, $\theta_r = 0.218$, $n = 2.76$, $\alpha = 2.0(\text{m}^{-1})$, $K_s = 0.316$ m/day). In all the simulations, the domain size was 6.0 m, spatial increment

was $\Delta z = 0.02$ m and uniform, and the lower boundary was assumed to be a free drainage (zero pressure gradient). The accuracy of the proposed methods was evaluated by comparing their mass-balance errors and pressure head profiles with those obtained by the traditional methods. The results indicated that the mass-balance errors of all the methods, provided they converged, were in 10^{-5} order of magnitude or less. Therefore, the mass-balance errors will not be presented. All the simulations were run on a Sun Ultra 5 workstation and the CPU time reported is user's CPU time and measured in second.

3.1. Effectiveness of using different time steps

This example aimed to show the difficulties of using the standard method to solve the prescribed-flux boundary and the improvement of the proposed

Table 2

The CPU time of the basic methods and the z -methods for simulating infiltrations into the clay under a single set of infiltration rates (simulation time was 6 days) (F represents iteration failed to converge)

q (m/day)	Δt (day)	MPI	Newton	IMPI	ZMPI	Znewton	ZIMPI
0.02	0.005	F	70.5	F	41.3	70.3	40.6
	0.05	F	F	F	7.6	F	7.5
	0.5	F	F	F	4.6	F	3.5
0.04	0.005	F	74.3	F	43.0	74.1	42.4
	0.05	F	F	F	13.0	F	11.8
	0.5	F	F	F	20.6	F	5.9
0.06	0.005	F	F	F	55.1	92.1	54.0
	0.05	F	F	F	18.5	F	16.8
	0.5	F	F	F	F	F	7.0

Table 3

The CPU time of the basic methods and z-methods simulating infiltrations into the loam under a single set of infiltration rates (simulation time was 2.0 days) (*F* represents iteration failed to converge)

<i>q</i> (m/day)	Δt (day)	MPI	Newton	IMPI	ZMPI	Znewton	ZIMPI
0.1	0.0005	104.8	163.0	104.8	104.9	163.4	104.3
	0.05	4.0	3.4	<i>F</i>	4.2	3.4	2.8
	0.5	<i>F</i>	0.5		<i>F</i>	0.5	1.0
0.2	0.0005	139.1	240.2	140.3	138.9	240.3	138.8
	0.05	7.0	4.1	<i>F</i>	7.4	4.6	3.9
	0.5	<i>F</i>	0.5	<i>F</i>	<i>F</i>	0.7	0.5
0.3	0.0005	169.2	239.1	141.4	169.7	241.6	140.8
	0.05	10.3	4.2	<i>F</i>	10.7	4.8	5.9
	0.5	<i>F</i>	0.7	<i>F</i>	<i>F</i>	1.9	1.3

method, using a wide range of time steps. We adopted a very dry initial condition (−100 m) in the sand and clay to show the difficulties, and a relatively wet initial condition (−1 m) in the loam to show that the proposed method does not give rise to extra errors. The reference pressure head, h_r , needed by the z-methods, was −0.1 m for the sand and −0.01 m for the clay and loam, higher than the pressure heads at the surface when $q = Q_N^{k+1}$. Tables 1–3 compare the CPU time of the basic methods and the z-methods for the three soils. The MPI and IMPI failed to converge, even using small time steps, for the sand and clay. The IMPI performs worse than the MPI for the loam, failing to converge when using relatively large time steps. This is due to the implicit treatment of the gravity

term in the IMPI that results in its $D_N^{k+1,m}$ and $B_N^{k+1,m}$ smaller than their counterparts in the MPI, which reduces the stability. The tables also show that in general, the application of the proposed method in the Newton method does not give an improvement. Therefore, in what follows the results of Znewton will not be presented.

The failure of the MPI and IMPI was due to the non-physical oscillation caused by their standard treatment of the flux boundary and the failure of the Newton method due to its non-diagonally dominant Jacobian matrix and the far-from-zero right-hand vector of the linear system. The improvement of ZMPI and ZIMPI lies in that they reduce such oscillation. As a sample to show this, Fig. 2 plots $\max|\delta h|$

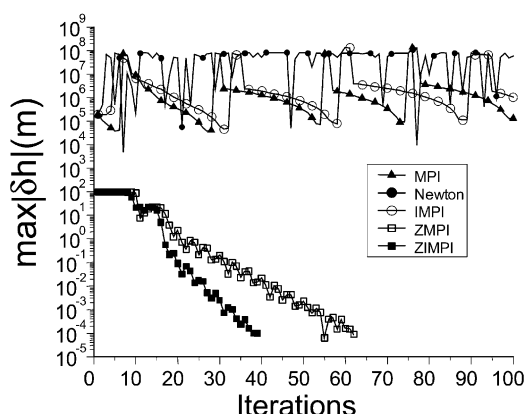


Fig. 2. $\max|\delta h|$ versus iterations of MPI, Newton, IMPI, ZMPI and ZIMPI using a time step of 0.005 days for simulating infiltration into the sand under the infiltration rate of 1.5 m/day.

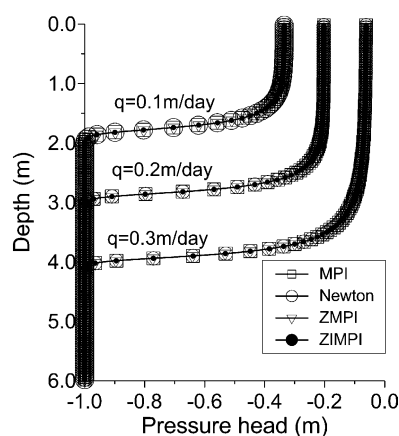


Fig. 3. Pressure head distributions after 2 days infiltration into the loam under the three infiltration rates, calculated by MPI, Newton, ZMPI and ZIIMPI using the same time step of 0.05 days.

Table 4

The impact of the reference h_r on the CPU time of the ZMPI and ZIMPI for simulating infiltrations into the three soils under constant infiltration rates, using $\Delta t = 0.0025$ days for the sand, and $\Delta t = 0.05$ days for the clay and loam (simulation time was 0.5 days for the sand, and 2.0 days for the loam and clay)

Soil	q (m/day)	ZMPI (m)			ZIMPI (m)		
		-0.1	-0.01	0.0	-0.1	-0.01	0.0
Sand	2.5	58.0	57.7	57.7	39.1	38.9	38.9
Clay	0.05	3.2	3.0	3.0	3.1	2.8	2.8
Loam	0.15	12.0	12.1	12.1	7.2	7.2	7.2

versus iterations of all the methods for simulating infiltration into the sand under the infiltration rate of 1.5 m/day, using a time step of 0.005 days. Fig. 3 compares the pressure head profiles in the loam under the three infiltration rates, calculated by all the methods using a time step of 0.05 days.

3.2. Sensitivity to the reference pressure head

This test aimed to show that the efficiency of the proposed method for the flux boundary is not very sensitive to the reference pressure head, h_r . The initial condition for all the examples in this test was a hydrostatic equilibrium that decreases upwards from zero at the bottom. The simulation time was 0.5 days for the sand, and 2.0 days for the clay and loam. The time

step for the sand was 0.0025 days, and for the clay and loam was 0.05 days. Table 4 compares the CPU time of the ZMPI and ZIMPI for the three soils, using three reference pressure heads. Clearly, the impact of the h_r on the computational cost is minor.

3.3. Effectiveness under temporally varying infiltration

This test was to show that the proposed method for the flux boundary is equally effective for solving flow under temporally varying infiltration rate that was given as $q = a[1 + \sin(bt)]$, where b controls the fluctuation of the infiltration rate. The three uniform soils and two layered soils: case A and case B each comprising two layers each layer 3.0 m thick, were

Table 5

CPU time of the all the methods for simulating flow under temporally varying infiltration rate into the three uniform soils and the two layered soils (simulation time was 0.4 days for the sand, 2.0 days for the loam, 6.0 days for the clay, 0.32 days for case A and 9.0 days for case B) (F represents iteration failed to converge)

Soil	q (m/day)	Δt (days)	MPI	Newton	IMPI	ZMPI	ZIMPI
Sand	$2[1 + \sin(10t)]$	0.001	F	F	F	75.6	58.9
		0.05	F	F	F	F	3.6
		0.1	F	F	F	F	2.4
Clay	$0.05[1 + \sin(4t)]$	0.005	F	59.7	F	F	69.1
		0.05	F	F	F	F	14.9
		0.1	F	4.8	F	F	9.2
Loam	$0.15[1 + \sin(4t)]$	0.005	F	F	F	32.1	29.2
		0.05	F	F	F	13.1	7.3
		0.1	F	F	F	13.9	4.3
Case A	$2[1 + \sin(10t)]$	0.001	F	F	F	61.4	47.7
		0.004	F	F	F	43.6	21.6
		0.04	F	F	F	F	4.3
Case B	$0.05[1 + \sin(2t)]$	0.01	F	49.7	F	F	59.4
		0.05	F	13.0	F	F	20.5
		0.2	F	F	F	F	4.0

Table 6

The impact of the van Genuchten parameters, n and α , on the CPU time of MPI, Newton and ZIMPI, using adaptive time-step and under-relaxation ($K_s = 0.35$ m/day, $\theta_s = 0.43$, $\theta_r = 0.11$, $\Delta t_{\min} = 10^{-6}$ day, $\Delta t_{\max} = 0.05$ days, $M = 15$, $\mu = 1.1$ and the simulation time was 6 days) (F represents iteration failed to converge)

	α (m ⁻¹)	n					
		1.5	1.8	2.4	3.0	3.6	4.2
MPI	1.01	F	24.4	28.3	33.4	38.0	40.7
	2.05	F	72.3	67.6	65.3	67.7	69.6
	4.08	F	F	91.1	82.0	82.3	80.4
	6.00	F	F	105.5	93.8	92.8	F
Newton	1.01	F	13.5	22.9	36.5	54.2	71.0
	2.05	F	46.2	79.8	106.0	130.9	150.5
	4.08	F	F	90.8	81.9	82.4	82.1
	6.00	F	F	194.2	211.6	F	F
ZIMPI	1.01	20.0	11.9	15.8	27.3	17.6	19.3
	2.05	31.6	27.0	25.1	25.3	21.3	21.1
	4.08	39.6	29.9	22.4	20.0	23.7	20.2
	6.00	34.8	25.3	20.4	21.2	22.5	32.7

studied. For case A the top layer was the sand and the bottom layer the loam, and for case B the top layer was the clay and the bottom layer the sand. The profile of case A gave rise to a perched water table. The initial condition for all the examples was the same as in Test 2, and the reference head needed in the ZMPI and ZIMPI was $h_r = 0.0$ m. The simulation time for case A was 0.32 days to ensure that a perched water table developed but no ponding occurred at the surface. Table 5 compares the CPU time of all the methods for each example.

3.4. Effectiveness of using adaptive time-step scheme for soils with different van Genuchten parameters n and α

This test aimed to show how the ZIMPI, a combination of the proposed method for the flux boundary and an improved method for the gravity term, improves the convergence over the MPI and Newton methods that treat the flux and the gravity term with standard methods. To test the robustness, we used an under-relaxation and an adaptive time-step scheme to simulate infiltration into soils with different combinations of van Genuchten parameters, n and α , which

represent the non-linear degree of soil hydraulic properties. The initial pressure head was a hydrostatic equilibrium that decreases upwards from zero at the bottom. The time step in all the methods was adjusted according to the convergence history. If the number of iterations in level k was less than M and the time step $\Delta t_k < \Delta t_{\max}$, then the time step in level $k + 1$ was increased to $\Delta t_{k+1} = \mu \Delta t_k$; otherwise it remained unchanged ($\Delta t_{k+1} = \Delta t_k$). If the iteration in level k failed to converge within M steps, the time step was halved and the iteration was re-launched for level k using the reduced time step; this procedure continued as long as $\Delta t_k > \Delta t_{\min}$ and the system was assumed to have failed to converge if the iteration could not converge within M steps using $\Delta t_k = \Delta t_{\min}$. A simple under-relaxation was also used. In all the three methods, the solution was updated by $h^{k+1,m+1} = \max[\min(h_r, h^{k+1,m} + \delta h^{k+1,m+1}), h_{\min}]$ in the iteration, where $\delta h^{k+1,m+1}$ is the solution of Eq. (13) and h_{\min} is the initial pressure head to keep the solution in the physical bounds. All the three methods started with the same time step of $\Delta t_1 = 0.0001$ day. In all the simulations, $\Delta t_{\max} = 0.05$ days, $\Delta t_{\min} = 10^{-6}$ days, $\mu = 1.1$, and the simulation time was 6.0 days. Table 6 compares the CPU time of the ZIMPI, MPI and the Newton method for simulating infiltration into each soil under a temporally varying infiltration rate of $q = 0.15[1 + \sin(t)]$.

4. Conclusions

A new method is proposed to handle the prescribed-flux boundary in numerical solution of water flow in variably saturated soils. The proposed method aims to reduce the iteration-to-iteration oscillation caused by the flux by providing a helpful feedback to the flux in the solution at the new iteration. In addition, we improve the implicit approach proposed by Zhang and Ewen (2000) for the gravity term by extending it to heterogeneous soils and approximating the inter-nodal hydraulic conductivity in the gravity term and the diffusive term with the same scheme. The improvement of the proposed methods was tested against the traditional Picard and Newton methods for a wide range of problems, including flow in homogeneous and heterogeneous soils under constant and temporally varying infiltration rate. The results

indicate that treating the diffusive term by the Picard iteration, the flux boundary and the gravity term by the proposed methods greatly improves the robustness and efficiency, allowing large time step to be taken without need of the under-relaxation, by which the traditional Picard and Newton methods often fail.

Acknowledgements

This work was funded by the Scottish Executive Environment and Rural Affairs Department as a part of Flexible Fund Scheme. We thank R.L. Cooley and the anonymous reviewer for their insightful and constructive comments, and suggestions to improve the manuscript.

Appendix A

Here we present a simple Newton iteration for the diffusive term, which is equivalent to the method of Li (1993), and that the Picard iteration for the diffusive term can be derived as a type of chord Newton iteration.

In the absence of the gravity term, the Richards' equation is written as follows with the Kirchhoff transformation:

$$\frac{\partial \theta}{\partial t} = \frac{\partial^2 \Phi}{\partial z^2} \quad (\text{A1})$$

where $\Phi(h) = \int_{-\infty}^h K(\xi) d\xi$ is the Kirchhoff transformation. For simplicity, we assume a uniform soil and discretize Eq. (A1) using a uniform spatial increment. The fully implicit finite-volume solution of Eq. (A1) is:

$$\Delta z \frac{\theta_i^{k+1} - \theta_i^k}{\Delta t} = \frac{\Phi_{i-1}^{k+1} - 2\Phi_i^{k+1} + \Phi_{i+1}^{k+1}}{\Delta z} \quad (\text{A2})$$

A.1. Newton iteration for the diffusive term

From the Kirchhoff transformation, the linear terms in the Taylor series expansion of $\Phi(h^{k+1,m+1})$ around

$h^{k+1,m}$ is

$$\begin{aligned} \Phi(h^{k+1,m+1}) &= \Phi(h^{k+1,m}) + \left. \frac{\partial \Phi}{\partial h} \right|^{k+1,m} \delta h^{k+1,m+1} \\ &= \Phi(h_i^{k+1,m}) + K(h^{k+1,m}) \delta h^{k+1,m+1} \end{aligned} \quad (\text{A3})$$

Applying this to Eq. (A2) gives:

$$\begin{aligned} \Phi_{i-1}^{k+1,m+1} &= \Phi(h_{i-1}^{k+1,m+1}) \\ &= \Phi(h_{i-1}^{k+1,m}) + \left. \frac{\partial \Phi}{\partial h} \right|_{i-1}^{k+1,m} \delta h_{i-1}^{k+1,m+1} \\ &= \Phi(h_{i-1}^{k+1,m}) + K(h_{i-1}^{k+1,m}) \delta h_{i-1}^{k+1,m+1}, \end{aligned}$$

$$\begin{aligned} \Phi_i^{k+1,m+1} &= \Phi(h_i^{k+1,m+1}) \\ &= \Phi(h_i^{k+1,m}) + \left. \frac{\partial \Phi}{\partial h} \right|_i^{k+1,m} \delta h_i^{k+1,m+1} \\ &= \Phi(h_i^{k+1,m}) + K(h_i^{k+1,m}) \delta h_i^{k+1,m+1}, \end{aligned}$$

$$\begin{aligned} \Phi_{i+1}^{k+1,m+1} &= \Phi(h_{i+1}^{k+1,m+1}) \\ &= \Phi(h_{i+1}^{k+1,m}) + \left. \frac{\partial \Phi}{\partial h} \right|_{i+1}^{k+1,m} \delta h_{i+1}^{k+1,m+1} \\ &= \Phi(h_{i+1}^{k+1,m}) + K(h_{i+1}^{k+1,m}) \delta h_{i+1}^{k+1,m+1} \end{aligned} \quad (\text{A4})$$

From Eq. (3), we have

$$\begin{aligned} \Phi_{i\pm 1}^{k+1,m} - \Phi_i^{k+1,m} &= \frac{1}{h_{i\pm 1}^{k+1,m} - h_i^{k+1,m}} \int_{h_i^{k+1,m}}^{h_{i\pm 1}^{k+1,m}} K(h) dh (h_{i\pm 1}^{k+1,m} - h_i^{k+1,m}) \\ &= K_{i\pm 1/2}^{k+1,m} (h_{i\pm 1}^{k+1,m} - h_i^{k+1,m}) \end{aligned} \quad (\text{A5})$$

Therefore, the Newton iteration for the diffusive

term is:

$$\frac{\Phi_{i-1}^{k+1,m+1} - 2\Phi_i^{k+1,m+1} + \Phi_{i+1}^{k+1,m+1}}{\Delta z} = \frac{K_{i-1/2}^{k+1,m}(h_{i-1}^{k+1,m} - h_i^{k+1,m}) + K_{i+1/2}^{k+1,m}(h_{i+1}^{k+1,m} - h_i^{k+1,m})}{\Delta z} + \frac{K(h_{i-1}^{k+1,m})\delta h_{i-1}^{k+1,m+1} - 2K(h_i^{k+1,m})\delta h_i^{k+1,m+1} + K(h_{i+1}^{k+1,m})\delta h_{i+1}^{k+1,m+1}}{\Delta z} \tag{A6}$$

A.2. Derivation of the Picard iteration as a type of ‘chord Newton’ iteration

The chord Newton iteration approximates the derivative in Eq. (A3) with a chord approach:

$$\frac{\partial \Phi}{\partial h} \Big|^{k+1,m} \approx \frac{\Phi(h^{k+1,m}) - \Phi(h^{k+1,m} - \varepsilon)}{\varepsilon} \approx \frac{\Phi(h^{k+1,m}) - \Phi(h^{k+1,m} + \varepsilon)}{-\varepsilon} \tag{A7}$$

where ε is a perturbation. Approximate the derivatives in Eq. (A4) by the following chord-slopes:

$$\begin{aligned} \frac{\partial \Phi}{\partial h} \Big|_{i-1}^{k+1,m} &= \frac{\Phi(h_{i-1}^{k+1,m}) - \Phi(h_{i-1}^{k+1,m} - \varepsilon_{i-1})}{\varepsilon_{i-1}}, \\ \frac{\partial \Phi}{\partial h} \Big|_i^{k+1,m} &= \frac{1}{2} \left[\frac{\Phi(h_i^{k+1,m}) - \Phi(h_i^{k+1,m} + \varepsilon_{i-1})}{-\varepsilon_{i-1}} + \frac{\Phi(h_i^{k+1,m}) - \Phi(h_i^{k+1,m} + \varepsilon_{i+1})}{-\varepsilon_{i+1}} \right], \\ \frac{\partial \Phi}{\partial h} \Big|_{i+1}^{k+1,m} &= \frac{\Phi(h_{i+1}^{k+1,m}) - \Phi(h_{i+1}^{k+1,m} - \varepsilon_{i+1})}{\varepsilon_{i+1}} \end{aligned} \tag{A8}$$

and choose $\varepsilon_{i-1} = h_{i-1}^{k+1,m} - h_i^{k+1,m}$, $\varepsilon_{i+1} = h_{i+1}^{k+1,m} - h_i^{k+1,m}$. Substituting Eq. (A8) into Eq. (A4) gives

$$\begin{aligned} \Phi_{i-1}^{k+1,m+1} - 2\Phi_i^{k+1,m+1} + \Phi_{i+1}^{k+1,m+1} &= (\Phi_{i-1}^{k+1,m} - 2\Phi_i^{k+1,m} + \Phi_{i+1}^{k+1,m}) \\ &+ \left\{ \frac{\Phi(h_{i-1}^{k+1,m}) - \Phi[h_{i-1}^{k+1,m} - (h_{i-1}^{k+1,m} - h_i^{k+1,m})]}{h_{i-1}^{k+1,m} - h_i^{k+1,m}} \delta h_{i-1}^{k+1,m+1} \right. \\ &- \left. \frac{\Phi(h_i^{k+1,m}) - \Phi[h_i^{k+1,m} + (h_{i-1}^{k+1,m} - h_i^{k+1,m})]}{-(h_{i-1}^{k+1,m} - h_i^{k+1,m})} \delta h_i^{k+1,m+1} \right\} \\ &+ \left\{ \frac{\Phi(h_{i+1}^{k+1,m}) - \Phi[h_{i+1}^{k+1,m} - (h_{i+1}^{k+1,m} - h_i^{k+1,m})]}{h_{i+1}^{k+1,m} - h_i^{k+1,m}} \delta h_{i+1}^{k+1,m+1} \right. \\ &- \left. \frac{\Phi(h_i^{k+1,m}) - \Phi[h_i^{k+1,m} + (h_{i+1}^{k+1,m} - h_i^{k+1,m})]}{-(h_{i+1}^{k+1,m} - h_i^{k+1,m})} \delta h_i^{k+1,m+1} \right\} \end{aligned} \tag{A9}$$

By expanding $\delta h^{k+1,m+1}$, the second term on the right-hand side of Eq. (A9) is

$$\begin{aligned}
& \frac{\Phi\left(h_{i-1}^{k+1,m}\right) - \Phi\left(h_i^{k+1,m}\right)}{h_{i-1}^{k+1,m} - h_i^{k+1,m}} \left(h_{i-1}^{k+1,m+1} - h_i^{k+1,m}\right) \\
& + \frac{\Phi\left(h_i^{k+1,m}\right) - \Phi\left(h_{i-1}^{k+1,m}\right)}{\left(h_{i-1}^{k+1,m} - h_i^{k+1,m}\right)} \left(h_i^{k+1,m+1} - h_i^{k+1,m}\right) \\
& = \frac{\Phi\left(h_{i-1}^{k+1,m}\right) - \Phi\left(h_i^{k+1,m}\right)}{h_{i-1}^{k+1,m} - h_i^{k+1,m}} \left[\left(h_{i-1}^{k+1,m+1} - h_i^{k+1,m+1}\right) - \left(h_{i-1}^{k+1,m} - h_i^{k+1,m}\right) \right] \\
& = \frac{\Phi\left(h_{i-1}^{k+1,m}\right) - \Phi\left(h_i^{k+1,m}\right)}{h_{i-1}^{k+1,m} - h_i^{k+1,m}} \left(h_{i-1}^{k+1,m+1} - h_i^{k+1,m+1}\right) - \left[\Phi\left(h_{i-1}^{k+1,m}\right) - \Phi\left(h_i^{k+1,m}\right) \right]
\end{aligned} \tag{A10}$$

Similarly, the third term on the right-hand side of Eq. (A9) is

$$\begin{aligned}
& \frac{\Phi\left(h_{i+1}^{k+1,m}\right) - \Phi\left(h_i^{k+1,m}\right)}{h_{i+1}^{k+1,m} - h_i^{k+1,m}} \left(h_{i+1}^{k+1,m+1} - h_{i+1}^{k+1,m}\right) \\
& + \frac{\Phi\left(h_i^{k+1,m}\right) - \Phi\left(h_{i+1}^{k+1,m}\right)}{\left(h_{i+1}^{k+1,m} - h_i^{k+1,m}\right)} \left(h_i^{k+1,m+1} - h_i^{k+1,m}\right) \\
& = \frac{\Phi\left(h_{i+1}^{k+1,m}\right) - \Phi\left(h_i^{k+1,m}\right)}{h_{i+1}^{k+1,m} - h_i^{k+1,m}} \left(h_{i+1}^{k+1,m+1} - h_i^{k+1,m+1}\right) - \left[\Phi\left(h_{i+1}^{k+1,m}\right) - \Phi\left(h_i^{k+1,m}\right) \right]
\end{aligned} \tag{A11}$$

Substituting Eqs. (A10) and (A11) into Eq. (A9) gives:

$$\begin{aligned}
& \Phi_{i-1}^{k+1,m+1} - 2\Phi_i^{k+1,m+1} + \Phi_{i+1}^{k+1,m+1} \\
& = \frac{\Phi\left(h_{i-1}^{k+1,m}\right) - \Phi\left(h_i^{k+1,m}\right)}{h_{i-1}^{k+1,m} - h_i^{k+1,m}} \left(h_{i-1}^{k+1,m+1} - h_i^{k+1,m+1}\right) \\
& + \frac{\Phi\left(h_{i+1}^{k+1,m}\right) - \Phi\left(h_i^{k+1,m}\right)}{h_{i+1}^{k+1,m} - h_i^{k+1,m}} \left(h_{i+1}^{k+1,m+1} - h_i^{k+1,m+1}\right) \\
& = K_{i-1/2}^{k+1,m} \left(h_{i-1}^{k+1,m+1} - h_i^{k+1,m+1}\right) \\
& + K_{i+1/2}^{k+1,m} \left(h_{i+1}^{k+1,m+1} - h_i^{k+1,m+1}\right)
\end{aligned} \tag{A12}$$

This proves that the Picard iteration for the diffusive term can be derived from a type of chord Newton iteration. Such iteration does not have the quadratic convergence rate near the solution that the full Newton iteration has, but converges faster than linearly.

References

- Celia, M.A., Bouloutas, E.T., Zarba, R.L., 1990. A general mass conservative numerical solution for the unsaturated flow equation. *Water Resour. Res.* 26, 1483–1496.
- Cooley, R.L., 1983. Some new procedures for numerical solution of variably saturated flow problems. *Water Resour. Res.* 19, 1271–1285.
- Forsyth, P.A., Wu, Y.S., Pruess, K., 1995. Robust numerical methods for saturated-unsaturated flow with dry initial conditions in heterogeneous media. *Adv. Water Resour.* 18, 25–38.
- van Genuchten, M.T., 1980. A closed form equation for predicting the hydraulic conductivity of unsaturated soil. *Soil Sci. Soc. Am. J.* 44, 892–898.
- Hills, R.G., Porro, I., Hudson, D.B., Wierenga, P.J., 1989. Modeling one-dimensional infiltration into very dry soils 1. Model development and evaluation. *Water Resour. Res.* 25, 1259–1270.
- Li, C.W., 1993. A simplified Newton iteration method with linear finite elements for transient unsaturated flow. *Water Resour. Res.* 29, 965–971.
- Miller, C.T., Williams, G.A., Kelley, C.T., Tocci, M.D., 1998. Robust solution of Richards' equation for non-uniform porous media. *Water Resour. Res.* 34, 2599–2610.
- Neuman, S.P., 1973. Saturated-unsaturated seepage by finite elements. *J. Hydraul. Div. Am. Soc. Civ. Engng* 99 (HY12), 2233–2250.
- Pan, L., Wierenga, P.J., 1995. A transformed pressure head-based

- approach to solve Richards' equation for variably saturated soils. *Water Resour. Res.* 31, 925–931.
- Pan, L., Wierenga, P.J., 1997. Improving numerical modelling of two-dimensional water flow in variably saturated, heterogeneous porous media. *Soil Sci. Soc. Am. J.* 61, 335–346.
- Paniconi, C., Putti, M., 1994. A comparison of Picard and Newton iteration in the numerical solution of multidimensional variably saturated flow problems. *Water Resour. Res.* 30, 3357–3374.
- Richards, L.A., 1931. Capillary conduction of liquids through porous mediums. *Physics* 1, 318–333.
- Ross, P.J., 1990. Efficient numerical methods for infiltration using Richards' equation. *Water Resour. Res.* 26, 279–290.
- Tocci, M.D., Kelley, C.T., Miller, C.T., 1997. Accurate and economical solution of the pressure-head form Richards' equation by the method of lines. *Adv. Water Resour.* 20, 1–14.
- Williams, G.A., Miller, C.T., 1999. An evaluation of temporally adaptive transformation approaches for solving Richards' equation. *Adv. Water Resour.* 22, 831–840.
- Williams, G.A., Miller, C.T., Kelley, C.T., 2000. Transformation approaches for simulating flow in variably saturated porous media. *Water Resour. Res.* 36, 923–934.
- Zaidel, J., Russo, D., 1992. Estimation of finite difference interblock conductivities for simulation of infiltration into initially dry soils. *Water Resour. Res.* 28, 2285–2295.
- Zhang, X., Ewen, J., 2000. Efficient method for simulating gravity-dominated water flow in unsaturated soils. *Water Resour. Res.* 36, 2777–2780.